TITLE PAGE

Citation Format: L. Colombo, M. Pagliazzi, S. Konugolu-Venkata-Sekar, D. Contini, T.Durduran, A. Pifferi, "In vivo time-domain diffuse correlation spectroscopy at 1μm," Proc. SPIE 11639, Optical Tomography and Spectroscopy of Tissue XIV,1163911 (5 March 2021); doi: 10.1117/12.2578443

DOI abstract link:

https://doi.org/10.1117/12.2578443

PROCEEDINGS OF SPIE

SPIEDigitalLibrary.org/conference-proceedings-of-spie

In vivo time-domain diffuse correlation spectroscopy at 1 μm

Colombo, L., Pagliazzi, M., Konugolu-Venkata-Sekar, S., Contini, D., Durduran, T., et al.

L. Colombo, M. Pagliazzi, S. Konugolu-Venkata-Sekar, D. Contini, T. Durduran, A. Pifferi, "In vivo time-domain diffuse correlation spectroscopy at 1 μm," Proc. SPIE 11639, Optical Tomography and Spectroscopy of Tissue XIV, 1163911 (5 March 2021); doi: 10.1117/12.2578443

SPIE.

Event: SPIE BiOS, 2021, Online Only

In vivo time-domain diffuse correlation spectroscopy at 1 μm

L. Colombo[1,*], M. Pagliazzi[2], S. Konugolu Venkata Sekar[1], D. Contini[1], T. Durduran[2,4], and A. Pifferi[1,3]

[1]*Politecnico di Milano, Dipartimento di Fisica, 20133 Milano, Italy*
[2]*ICFO-Institut de Ciències Fotòniques, The Barcelona Institute of Science and Technology, 08860 Castelldefels (Barcelona), Spain*
[3]*Istituto di Fotonica e Nanotecnologie, Consiglio Nazionale delle Ricerche, 20133 Milano, Italy*
[4]*Institució Catalana de Recerca i Estudis Avançats (ICREA), 08015 Barcelona, Spain*
**email: lorenzo.colombo@polimi.it*

Abstract: Diffuse correlation spectroscopy (DCS) is an optical technique which, by studying the speckle intensity fluctuations of coherent light diffused in a turbid medium, retrieves information regarding the scatterers motion. In the case of biological tissues, the particles of interest are the red blood cells, from which is possible to measure non-invasively microvascular blood flow (BF). However, being based on a continuous-wave light source, depth discrimination is achievable only by using multiple source-detector separations. On the other hand, time-domain (TD) DCS is a novel approach which exploits a pulsed yet coherent light source to discriminate the intensity fluctuations at different photon time-of-flights. This additional information is beneficial for in vivo applications, due to the physical relationship between photon time-of-flight and mean depth penetration. TD-DCS is typically performed in the spectral range between 700 and 800 nm. Here, we explore TD-DCS in a new spectral range compared to the typical one, moving to the spectral region beyond the water absorption peak (i.e., >970 nm). We performed liquid phantom and in vivo experiments on the human muscle at a wavelength of 1000 nm. Also, the possible advantages in terms of depth sensitivity and signal-to-noise ratio are discussed.

INTRODUCTION AND METHODS

Diffuse correlation spectroscopy (DCS) is a non-invasive optical technique that, by studying the intensity fluctuations of coherent light diffused by a turbid medium, extracts information regarding the scatters motion. In the case of biological tissues, the moving scatterers are mainly red blood cells, thus it is possible to measure microvascular blood flow (BF) in a non-invasive way. A DCS experiment is typically performed in reflectance geometry, at a source-detector separation of few centimeters (2-3 cm) [1], [2]. However, since a continuous-wave source is used, depth discrimination is achievable only by using multiple SD separations. A novel approach is time-domain (TD) DCS, which uses a pulsed yet temporally coherent light source to measure the intensity auto-correlations at different photon time-of-flights [3]–[6]. Due to the physical relationship between photon time-of-flight and its mean penetration depth, this can improve the BF depth discrimination even when a single SD separation is used [7], [8]. The aim of this work is to explore TD-DCS at wavelengths beyond the water absorption peak (> 970 nm). This may be beneficial in terms of depth sensitivity and signal-to-noise ratio.

Our experimental setup, for details see Ref. [9], is based on a custom Ti:Sapphire mode-locked laser, tuned to a pulse width of 200 ps full-width at half-maximum. The laser light was injected in the tissue with a 100 μm core diameter graded-index fiber and the diffused light was recollected, at a SD separation $\rho = 1$ cm in reflectance, with a 4.4 μm core diameter single-mode fiber (780HP, Thorlabs, Germany). The photon arrival times were measured with a InGaAs photomultiplier (H10330-25 Hamamatsu Photonics, Japan) together with a time correlated single

Optical Tomography and Spectroscopy of Tissue XIV, edited by Sergio Fantini, Paola Taroni, Proc. of SPIE
Vol. 11639, 1163911 · © 2021 SPIE · CCC code: 1605-7422/21/$21 · doi: 10.1117/12.2578443

photon counting board (TimeHarp 260 pico, PicoQuant, Germany), and the intensity auto-correlations were computed via software.

RESULTS AND DISCUSSION

We first performed liquid phantom experiments based on the recipe in Ref. [10]. To prepare the phantom, we mixed 5% of intralipid20 (B. Braun Melsungen, Germany) to distilled water, for comparing the auto-correlation functions measured at a typically used wavelength (785 nm) with a longer one (1000 nm). Both the measurements had 1 s sampling time (1 Hz) and a total duration of 300 s.

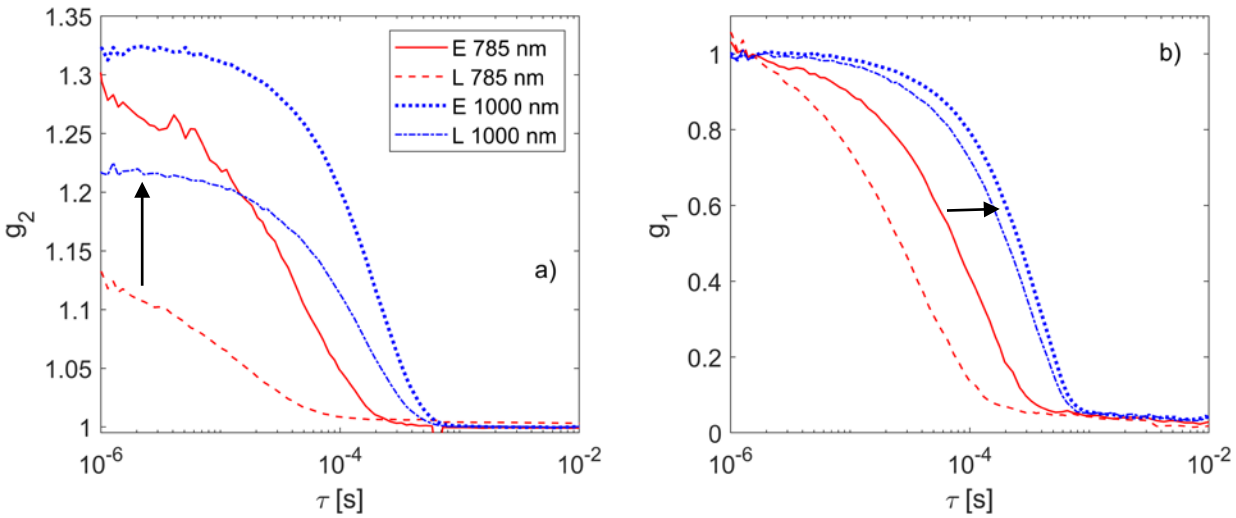

Figure 1: Liquid phantom a) intensity (g2) and (b) electric-field (g1) auto-correlation functions, measured at 785 nm and 1000 nm, for an early and a late temporal gate. The main differences observed are an increase of the β parameter (i.e., amplitude of g2) and a slower decay rate.

Moving to the longer wavelength the g_1 auto-correlation decay time (i.e., point where the measured electric field auto-correlation falls below 0.5) moved from 45 ± 2 μs to 217 ± 16 μs (MEAN ± SD) for ungated acquisition, almost 5 times slower. This effect was observed also for the gated autocorrelation [Fig1(b)]. In addition, from the measured g_2 curves [Fig1(a)] we observed an increase of the β parameter, for both the early and the late gate.

Then, we performed *in vivo* cuff occlusion experiments on the forearm muscle of 4 adult subjects. The protocol had a duration of 10 min and was composed of 3 min of baseline, 3 min of occlusion with a tourniquet inflated at a 200-mmHg pressure to induce an arterial occlusion, and 4 min of recovery after the deflation. Figure 2 reports a comparison of the baseline intensity (g_2) and electric-field (g_1) auto-correlation functions, for a subject with 2.7 mm thickness of the superficial layer, measured at the two wavelengths for two different temporal gates (early and late). As for the case of the phantom experiment, moving to the longer wavelength we observed in the autocorrelations a higher value of the coherence parameter β and a slower decay rate.

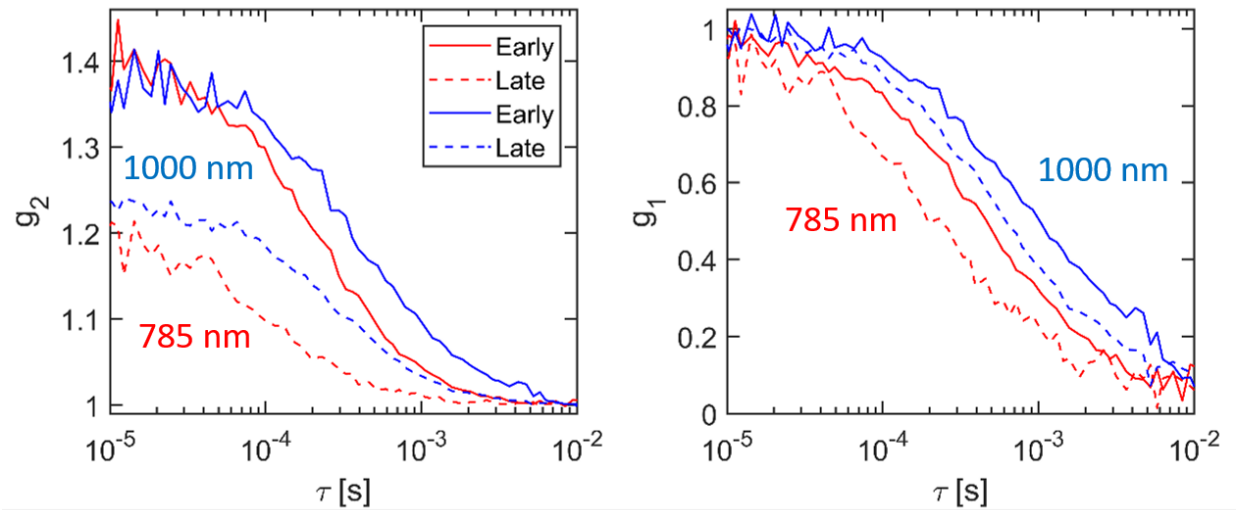

Figure 2: Cuff occlusion experiment baseline auto-correlation functions (5 s averaging time): a) intensity auto-correlations (g_2) and b) electric-field auto-correlations (g_1). The figure compares the early gate (continuous lines) and late gate (dashed lines) auto-correlation measured at 785 nm (red) and 1000 nm (blue).

In Table 1 we report for each subject the thickness of the superficial layer, the optical properties, and the count rate, and baseline BFI both for gated and ungated acquisition. In Figure 3 we report the results of the cuff occlusion experiment for all the 4 subjects with 1 Hz acquisition rate. We show the absolute BFI time traces for the early and the late time gate. Details for the data analysis can be found in Ref. [11].

Table 1: Results of the cuff occlusion experiment at 1000 nm. The optical properties were measured with a time resolved diffuse optical spectrometer. The reported count rate and BFI are the average values measured at baseline.

Subject	Superficial thickness [mm]	μ_a [cm^{-1}]	μ_s' [cm^{-1}]	Count rate [kcps]	BFI [10^{-9} cm^2/s]		
					Early	Late	Ungated
1	2.7	0.52	7.7	151 ± 3	3.1 ± 0.4	3.0 ± 0.4	3.0 ± 0.36
2	4.8	0.25	7.9	263 ± 9	1.2 ± 0.24	1.3 ± 0.2	1.1 ± 0.2
3	6.5	0.22	8.9	336 ± 7	0.63 ± 0.07	0.72 ± 0.06	0.59 ± 0.05
4	2.2	0.49	7.8	112 ± 11	1.2 ± 0.25	1.3 ± 0.31	1.2 ± 0.2

As shown in Figure 3, the BFI has different time trends depending on the specific subject. In particular, the hyperemic peak after the release has a quite large inter-subject variability. This effect might be related to the differences in superficial thickness and optical properties between the subjects. Also, the baseline BFI show quite different values across the volunteers. We note that the small differences between the early and the late gate might be due to the limited value of the superficial thickness of the subjects.

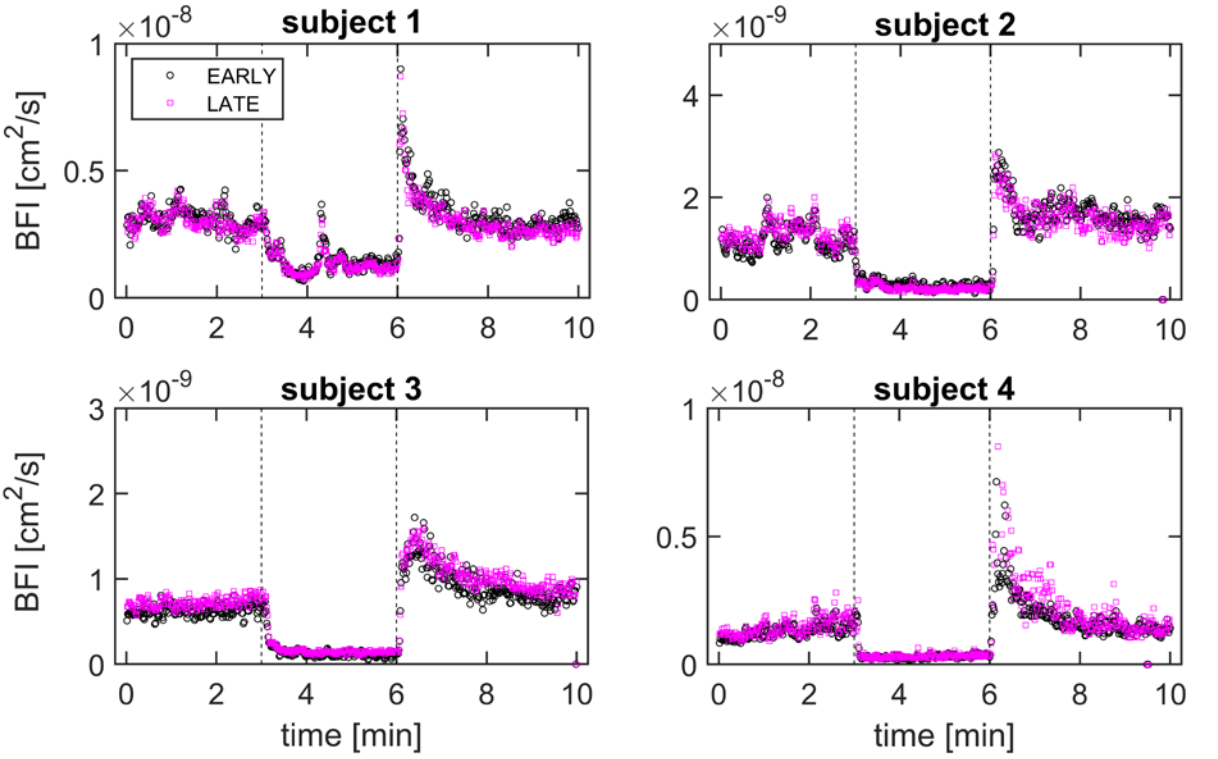

Figure 3: Blood flow index time traces of the cuff occlusion experiment, for an early gate (black circles) and a late gate (magenta squares). The vertical dashed lines enclose the time interval when the occlusion was performed, from minute 3 to minute 6 for all the subjects, inflating the torniquet at a 200-mmHg pressure.

In conclusion, we reported the first to our knowledge TD-DCS experiment beyond the water absorption peak (i.e., > 970 nm). We demonstrated the feasibility of the experiments for both phantom and in vivo experiments. Acquisition rates up to 1 Hz were achieved with the current setup. However, by moving to even longer wavelengths it might be possible to decrease the tissue attenuation thus increasing the signal-to-noise ratio and depth sensitivity.

Acknowledgments: The authors acknowledge financial support from the European Union's H2020 programs LASERLAB-EUROPE V (n. 871124) and LUCA (n. 688303, H2020-ICT-2015) and Marie Skłodowska-Curie Innovative Training Network (ITN-ETN) BITMAP (n. 675332).

References

[1] D. A. Boas and A. G. Yodh, "Spatially varying dynamical properties of turbid media probed with diffusing temporal light correlation," *J. Opt. Soc. Am. A*, vol. 14, no. 1, pp. 192–215, 1997.

[2] T. Durduran, R. Choe, W. B. Baker, and A. G. Yodh, "Diffuse optics for tissue monitoring and tomography," *Reports Prog. Phys.*, vol. 73, p. 076701, 2010.

[3] M. Pagliazzi *et al.*, "Time domain diffuse correlation spectroscopy with a high coherence pulsed source: in vivo and phantom results," *Biomed. Opt. Express*, vol. 8, no. 11, p. 5311, 2017.

[4] M. Pagliazzi *et al.*, "In vivo time-gated diffuse correlation spectroscopy at quasi-null source-detector separation," *Opt. Lett.*, vol. 43, no. 11, p. 2450, Jun. 2018.

[5] J. Sutin *et al.*, "Time-domain diffuse correlation spectroscopy," *Optica*, vol. 3, no. 9, p. 1006, 2016.

[6] D. Tamborini *et al.*, "Portable system for Time-Domain Diffuse Correlation Spectroscopy," *IEEE Trans. Biomed. Eng.*, vol. 66, no. 11, p. 3014, 2019.

[7] A. Torricelli *et al.*, "Time domain functional NIRS imaging for human brain mapping," *NeuroImage*. 2014.

[8] L. Spinelli, A. Farina, T. Binzoni, A. Torricelli, A. Pifferi, and F. Martelli, "There's plenty of light at the bottom: statistics of photon penetration depth in random media," in *Scientific Reports*, 2016, vol. 6, p. srep27057.

[9] L. Colombo, M. Pagliazzi, S. Konugolu Venkata Sekar, D. Contini, T. Durduran, and A. Pifferi, "In vivo time-domain diffuse correlation spectroscopy above the water absorption peak," *Opt. Lett.*, 2020.

[10] L. Cortese *et al.*, "Liquid phantoms for near-infrared and diffuse correlation spectroscopies with tunable optical and dynamic properties," *Biomed. Opt. Express*, vol. 9, no. 5, p. 2068, May 2018.

[11] L. Colombo *et al.*, "Effects of the instrument response function and the gate width in time-domain diffuse correlation spectroscopy: model and validations," *Neurophotonics*, vol. 6, no. 03, p. 1, 2019.